Thermal Analysis of Ethylene–Propylene Copolymer-*Grafted*-Glycidyl Methacrylate

XIAOMIN ZHANG, LIXIA LI, ZHIHUI YIN, YUCHEN QI, and JINGHUA YIN*

Polymer Physics Laboratory, Changchun Institute of Applied Chemistry, Chinese Academy of Sciences, Changchun 130022, People's Republic of China

SYNOPSIS

The thermal properties of ethylene–propylene copolymer grafted with glycidyl methacrylate (EP-*g*-GMA) were investigated by using differential scanning calorimetry (DSC). Compared to the plain ethylene–propylene copolymer (EP), peak values of melting temperature (T_m) of the propylene sequences in the grafted EP changed a little, crystallization temperature (T_c) increased about 8–12°C, and melting enthalpy (ΔH_m) increased about 4–6 J/g. The isothermal and nonisothermal crystallization kinetics of grafted and ungrafted samples was carried out by DSC. Within the scope of the researched crystallization temperature, the Avrami exponent (n) of ungrafted sample is 1.6–1.8, and those of grafted samples are all above 2. The crystallization rates of propylene sequence in EP-*g*-GMA were faster than that in the plain EP and increased with increasing of grafted monomer content. It might be attributed to the results of rapid nucleation rate. © 1996 John Wiley & Sons, Inc.

INTRODUCTION

The development of new materials by polymer blending has become an increasingly important industrial activity because it is a way of modifing some basic properties of existing polymers. Generally, melt mixing of two polymers leads to a two-phase system because polymers are often thermodynamically immiscible. The resulting material exhibits poor properties as a result of a weak adhesion between two phases. Methods to improve phase adhesion between two immiscible components have been the subject of research activity.[1–12] In recent years, GMA has been reported as the grafting monomer of polyolefins, which can be functionalized as *in situ* compatibilizers of polymer alloys, such as polyolefins blended with polyamides and polyesters.[13–16]

The aim of this work is to study the influence of the grafted GMA in EP-*g*-GMA samples on their thermal properties, including melting and crystallization temperature, fusion enthalpy, crystallization kinetics, nucleating effect, etc.

* To whom correspondence should be addressed.

Journal of Applied Polymer Science, Vol. 62, 1933–1939 (1996)
 CCC 0021-8995/96/111933-07

EXPERIMENTAL

Materials

The low ethylene content ethylene-propylene copolymer (EP) was supplied by Liao Ning PanJin Natural Gas Chemical Co. (China), commercial model P340. Its melting flow index (MI) is about 1.0 g/10 min, and the C_2 content is 10%. EP-*g*-GMA samples were prepared by reaction extruding. The details of preparation and characterization were reported in a previous article.[17] The compositions and the degree of grafting of samples used in this work were listed in Table I.

Optical Microscopy Observation

Small samples were placed on a glass slide in a compression molder and heated to 200°C and held for 5 min. After melting, a coverslide placed over the sample was pressed down manually to produce a thin film; the resulting film was put on the hot stage. Before observation, the temperature of the hot stage was controlled 126°C for EP and 132°C for EP-*g*-GMA, and then isothermal crystallization was monitored. Growth of the spherulites of EP and

Table I The Compositions and The Grafting Degrees of Investigated Samples

Code	EP Content (%)	DCP Content (%)	GMA Content (%)	Grafting Degree (%)
A	100	0	0	0
B	100	0	4	0
C	100	0.1	2	0.29
D	100	0.1	4	0.54
E	100	0.1	6	0.77
F	100	0.1	8	0.81

EP-*g*-GMA was observed in an Universal R Pol polarizing microscope.

Thermal Analysis

A Perkin-Elmer DSC-II was used to research the thermal properties of EP and EP-*g*-GMA. The measurements of T_m, T_c, and ΔH_m were carried out under a nitrogen atmosphere using a heating and cooling rate of 10 K/min. The kinetic studies were also carried out by using calorimetric techniques. For isothermal crystallization experiments, the samples were heated about 10°C higher than their corresponding melting temperature and held for 10 min. Subsequently, the samples were cooled at a rate of 10 K/min to the desired temperatures. The corresponding thermograms were recorded as a function of time until the crystallization was completed. For the nonisothermal tests, samples were held at 473 K for 10 min to remove thermal history. The sample was then cooled at a rate of 5, 10, 20, 40, and 80 K/min to a final temperature of 300 K. Before the thermal analysis, all samples were extracted with boiling benzene to remove the unreacted monomer and GMA homopolymer. The pure EP was also treated with the same procedure.

RESULTS AND DISCUSSION

Analysis of Thermal Parameters

Melting temperature (T_m), crystallization temperature (T_c), and melting enthalpy (ΔH_m) of propylene sequences in EP and EP-*g*-GMA specimens were shown in Table II. Compared with the plain EP, T_m values of propylene crystals in EP-*g*-GMA decreased 1–2°C, and ΔH_m increased 4–6 J/g. The crystallization temperature of propylene sequence in EP-*g*-GMA increased 8–12°C. These results could be explained from the monomer grafted position. EP used in this work containes about 10% of ethylene. Grafting reactions occurred mainly on ethylene sequences.[18] Therefore, the grafted GMA molecules were preferentially bonded to ethylene sequences. The grafted GMA could act as a nucleation agent, which improved the crystallization capability of propylene sequences, and propylene sequences might crystallize at higher temperature.

Isothermal Crystallization

In this work, we assume that the crystallization behavior of EP and EP-*g*-GMA obeys the basic Avrami assumption, i.e., the crystallization of propylene sequences of EP and EP-*g*-GMA proceeds by radial growth from random nuclei until growing spherulites impinge with neighboring spherulites. The following optical microscopy provides the proof. Figure 1 shows the morphology of EP and EP-*g*-GMA isothermally crystallized from the melt. It is clearly seen that the growing spherulities of EP and EP-*g*-GMA have impinged with the neighbors. In the previous work of one of authors of this paper,[19] morphologies of ethylene-propylene copolymers with C_2-content of 88, 81, and 74 mol % (named as EP88,

Table II Melting Temperature (T_m), Crystallization Temperature (T_c), Melting Enthapy (ΔH_m), and ($T_m - T_c$) of Propylene Sequences for EP and Differentt GMA Contents of EP-*g*-GMA

Code	Grafting Degree (%)	T_m (°C)	T_c (°C)	ΔH_m (J/g)	$T_m - T_c$ (°C)
A	0	168.3	109.2	74.4	59.1
B	0	168.0	111.0	74.6	57.0
C	0.29	167.3	123.6	78.5	43.7
D	0.54	167.0	124.8	80.6	42.2
E	0.77	165.9	125.5	80.7	40.4

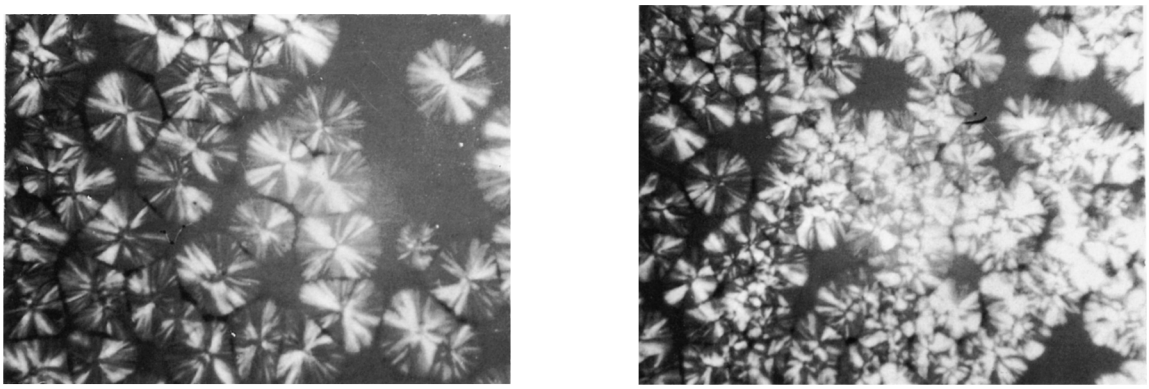

EP EP-g-GMA with GMA content 0.77%

Figure 1 Optical micrographs of EP and EP-*g*-GMA crystallized at 125 and 132°C, respectively.

EP81, and EP71) were studied. It was found that spherulites of propylene sequences of EP88 and EP81 copolymers were crystallized from random nuclei and grew by radial growth until impingement with neighbor spherulites took place. Hence, it can be considered that EP and EP-*g*-GMA obey the basic Avramic assumptions. It is reasonable to describe the isothermal crystallization of EP and EP-*g*-GMA by using the Avrami equation.

The Avrami equation for isothermal crystallization is represented as

$$1 - X_c = \exp(-Kt^n) \quad (1)$$

where X_c is the relative crystallinity by volume, k is the rate constant, and n is the Avrami exponent. K and n are determined by the conventional Avrami method. Figures 2 and 3 show Avrami plots with the isothermal DSC data obtained at various crystallization temperatures for EP and EP-*g*-GMA. It is easily seen in the Avrami plots that the Avrami equation describes the isothermal crystallization fairly well in the early stage. Because of curvature at the latter stage of crystallization, only the linear portion was used to estimate crystallization kinetics of investigated specimens. Some authors have attributed the curvature to secondary crystallization,[20] leading to isothermal lamellar thickening, nucleation and growth processes occurring simultaneously.[21] The kinetic parameters determined by the plot $\log[-\ln(1 - X_c)]$ against log are listed in Table III. The values of exponent n shown in Table III were not integral. This might be caused by such factors as mixed nucleation modes, secondary crystallization, or intermediate dimensionality of crystal

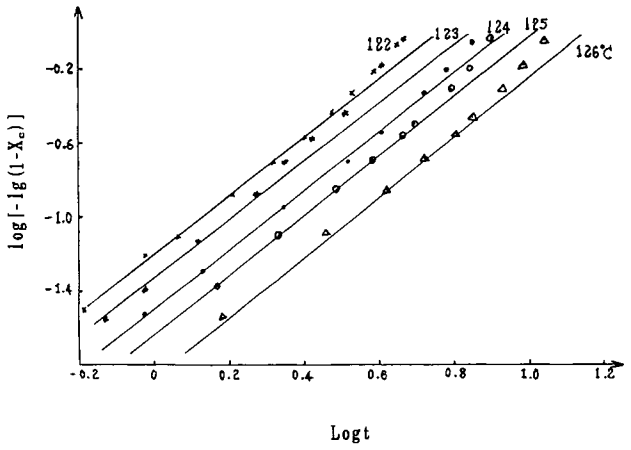

Figure 2 The AVRAMI plot of plain EP.

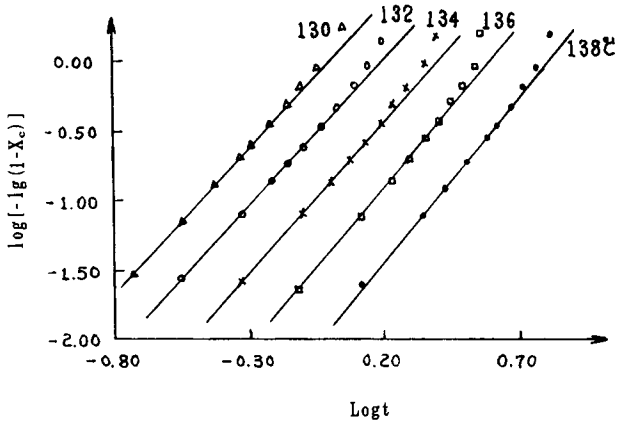

Figure 3 The AVRAMI plot of EP-*g*-GMA with a GMA content of 0.50%.

Table III Kinetic Parameters of EP and EP-*g*-GMA at Different Crystallization Temperatures (T_c)

Sample	Grafting Degree (%)	T_c (°C)	K (min^{-n})	n	$t_{1/2}$ (min)
EP	0	122	0.133	1.8	2.7
EP	0	123	0.102	1.8	3.6
EP	0	124	0.074	1.6	4.6
EP	0	125	0.052	1.6	5.0
EP	0	126	0.003	1.7	6.7
EP-*g*-GMA	0.29	130	0.179	2.05	1.9
EP-*g*-GMA	0.29	132	0.149	2.04	2.1
EP-*g*-GMA	0.29	134	0.084	2.12	2.7
EP-*g*-GMA	0.29	136	0.071	2.23	2.8
EP-*g*-GMA	0.29	138	0.028	2.29	4.0
EP-*g*-GMA	0.54	130	2.110	2.1	0.6
EP-*g*-GMA	0.54	132	0.650	2.1	1.0
EP-*g*-GMA	0.54	134	0.303	2.2	1.5
EP-*g*-GMA	0.54	136	0.970	2.3	2.4
EP-*g*-GMA	0.54	138	0.270	2.3	3.9
EP-*g*-GMA	0.77	130	2.260	2.1	0.6
EP-*g*-GMA	0.77	132	0.900	2.1	0.9
EP-*g*-GMA	0.77	134	0.307	2.3	1.4
EP-*g*-GMA	0.77	136	0.111	2.3	2.2
EP-*g*-GMA	0.77	138	0.036	2.4	3.4

growth.[22] The Avrami exponent n of pure EP was 1.7–1.8, and values of EP-*g*-GMA were all higher than 2. The higher content of GMA in EP-*g*-GMA, the higher the value n. It is well established that PP undergoes athermal nucleation.[23,24] The Avrami exponent for the athermally nucleated[25] and truncated sphere is in the range of 2 to 3. Truncated spheres are formed when spherulities impinged.

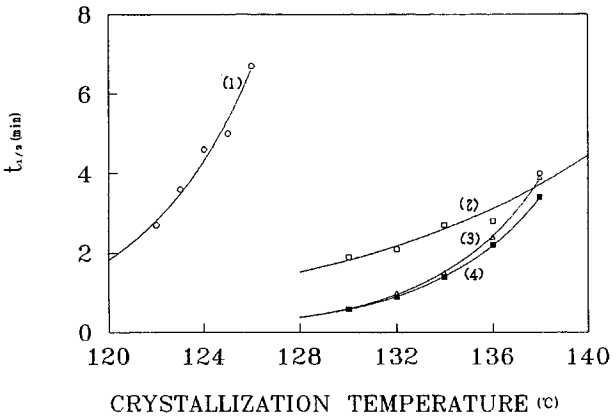

Figure 4 Plot of crystallization half-time against crystallization temperature: (1) EP; (2) EP-*g*-GMA with a GMA content of 0.26%, (3) EP-*g*-GMA with a GMA content of 0.54%, and (4) EP-*g*-GMA with a GMA content of 0.77%.

Crystallization rates of polymers can be expressed in terms of half time $t_{1/2}$, which defined as the time that it needs to fulfill the half crystallinity. The shorter the half time, the faster the crystallization rate, and vice versa. Figure 4 shows the changes of half time $t_{1/2}$, as a function of the crystallization temperature for the pure EP and EP-*g*-GMA. In all cases, $t_{1/2}$ increases exponentially at the higher crystallization temperature, confirming that the ordering process occurs through a nucleation mechanism.[26]

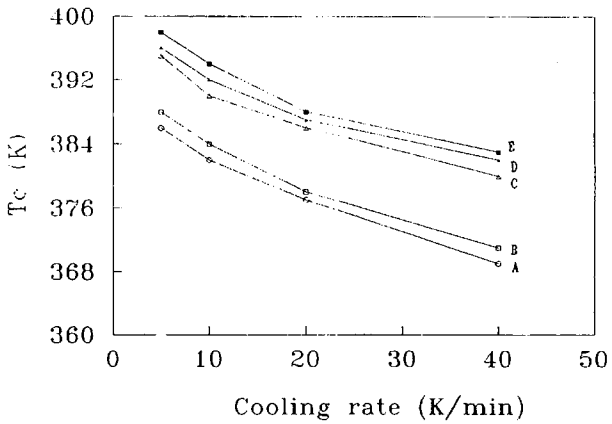

Figure 5 Effect of the grafting degree and cooling rate on crystallization temperature.

For the same crystallization temperature, the values of $t_{1/2}$ for high GMA content of EP-*g*-GMA are larger than that for low GMA content of EP-*g*-GMA. This behavior is related to the nucleating activity of glycidyl methacrylate in the crystallization of the EP. The experimentally accessible crystallization temperatures for grafted EP shown in Figure 4 are higher than those accessible for the ungrafted samples, which indicates that the grafted GMA induces an increase in the crystallization rate of propylene sequences; otherwise, the behavior of EP and EP-*g*-GMA should be identical.

According to Turndull–Fisher equation, the radial growth rate of polymer spherulities G is described as

$$G = G_o \cdot \exp[-\Delta F^o/KT]\exp[-\Delta\Phi^o/KT] \quad (2)$$

where ΔF^o is the free energy of formation of a surface nucleus of critical size, $\Delta\Phi^o$ the diffusional activation energy of crystallizing segments across the phase boundary, R the gas constant, and T the crystallization temperature in K. Using WLF theory,[27] ΔF^o can be expressed as following

$$\Delta F^o = 4120T_c/(51.6 + T_c - T_g) \quad (3)$$

where T_c is the crystallization temperature and T_g the glass transition temperature. In the present work, T_g for pure EP is almost equal to that of EP-*g*-GMA (272–274 K). Because the T_c of EP-*g*-GMA is higher than EP, we could conclude that ΔF^o of EP-*g*-GMA are higher than EP. When the radial growth rate was dominated by ΔF^o, the crystal growth rate of grafted EP are lower than EP.

Table IV The Ziabicki Exponent (n'') at Various Cooling Rates for EP and EP-*g*-GMA

Sample	Grafting Degree	Cooling Rate	n''
EP	0	5	3.71
EP	0	10	3.28
EP	0	20	3.01
EP	0	40	2.94
EP-*g*-GMA	0.29	5	4.42
EP-*g*-GMA	0.29	10	4.47
EP-*g*-GMA	0.29	20	4.12
EP-*g*-GMA	0.29	40	3.39
EP-*g*-GMA	0.54	5	4.45
EP-*g*-GMA	0.54	10	5.15
EP-*g*-GMA	0.54	20	4.32
EP-*g*-GMA	0.54	40	4.33
EP-*g*-GMA	0.77	5	4.77
EP-*g*-GMA	0.77	10	5.45
EP-*g*-GMA	0.77	20	4.80
EP-*g*-GMA	0.77	40	4.78

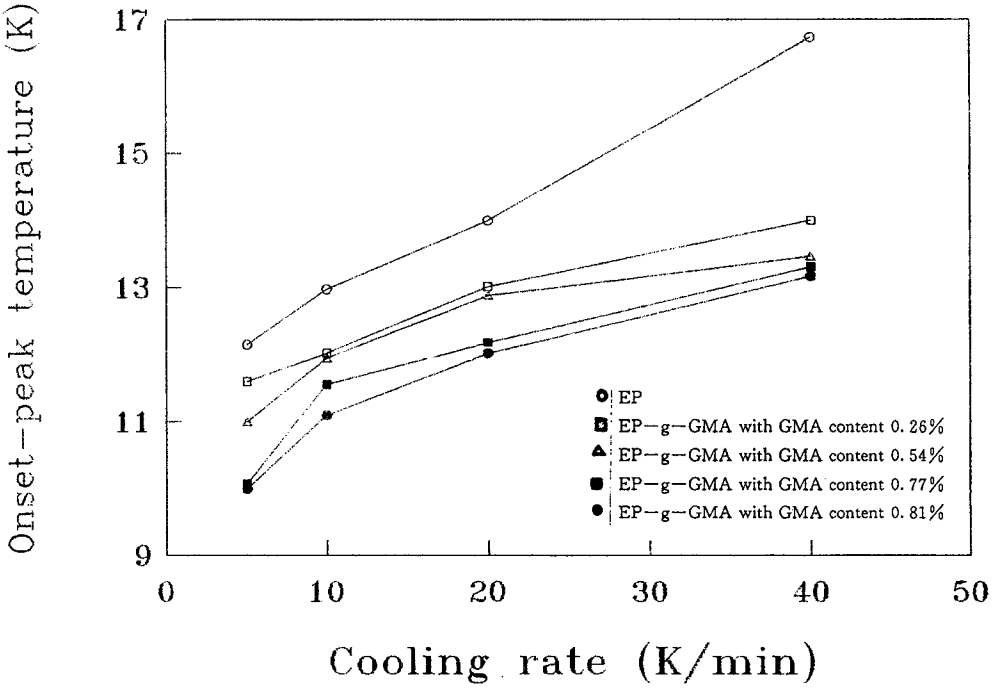

Figure 6 Effect of grafting degree on crystallization rate expressed by means of the difference between the onset temperature and the peak temperature.

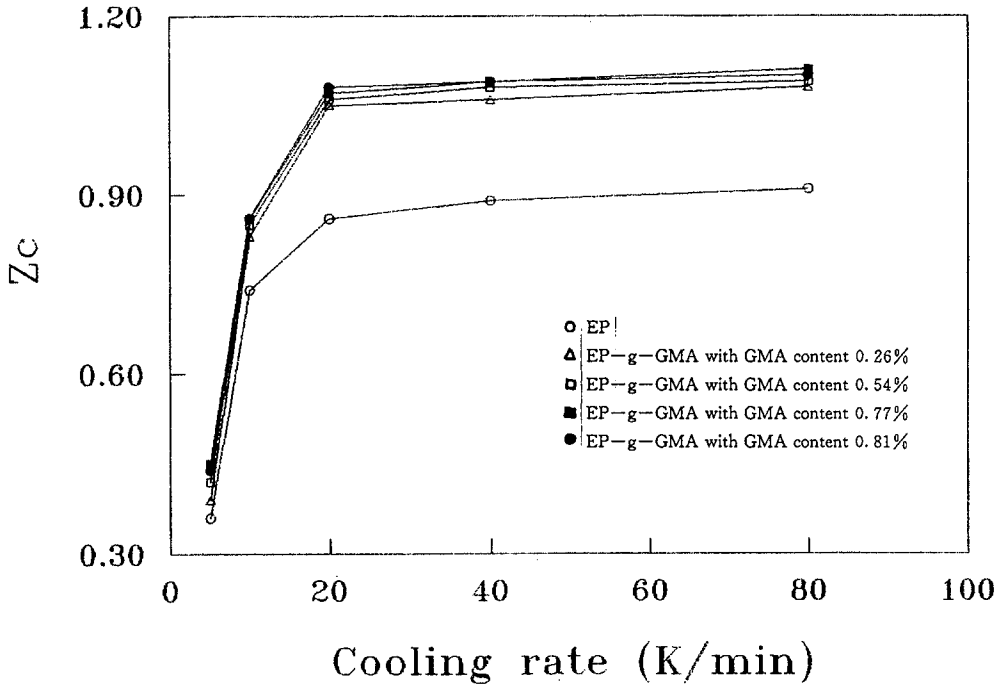

Figure 7 Effect of grafting degree and cooling rate on the Ziabicki rate constant.

The effect of $\Delta\Phi^o$ on the radial growth rate could be analyzed as follows. $\Delta\Phi^o$ is expressed as[28]

$$\Delta\Phi^o = T_m^O \cdot 4b_o \cdot \sigma \cdot \sigma_e / \Delta H_m (T_m^O - T_c) \qquad (4)$$

where b_o is the monolayer thickness, σ the lateral surface energy, σ_e the fold surface energy, ΔH_m the heat of fusion, and T_m^o the equilibrium melting temperature. From Table II, we know that the ΔH_m for EP-*g*-GMA is higher than EP only (4–6 J/g), and the equilibrium melting temperatures of propylene sequences for different ethylene contents was identical (210°C).[29] When the growth rate is dominated by the $\Delta\Phi^o$, from the eq. (4), we know the G value for EP-*g*-GMA is lower than EP. It is well known that crystallization rates were determined by the nucleation rate and crystal growth rate. From the above discussion, it is found that the overall crystallization rates of EP-*g*-GMA are higher than that of EP, and the radial growth rates of EP-*g*-GMA are lower than EP. Therefore, we can conclude that EP-*g*-GMA have more rapid nucleation rates than EP.

Nonisothermal Crystallization

Figure 5 shows the dependence of crystallization peak temperature on the cooling rate for various samples, we found that crystallization temperature of EP-*g*-GMA is about 10 K higher than the plain EP. It suggested that the degree of supercooling of EP-*g*-GMA is higher than pure EP.

Back and Ledbetter[30] suggested that the smaller the difference between the onset and the peak temperatures, the faster the overall crystallization rate. The onset temperature indicates the beginning of the crystallization process, while the maximum of the exotherm peak indicates the occurrence of spherulite impingement.[31] Figure 6 shows the difference between the onset and peak temperatures for representative samples. The difference is smaller for all grafted samples, indicating the grafted EP spherulities crystallized faster and impinged earlier than the nonfunctionalized EP. The overall crystallization rate is controlled by two mechanisms, namely, nucleation rate and growth rate. The grafted GMA onto EP molecule chain may increase the nucleation rate.

The Ziabicki analysis[32] is also an extension of the Avrami analysis to nonisothermal conditions. The kinetics of nonisothermal crystallization can be characterized by eq. (5).

$$\log[-\ln(1 - X(t))] = n''\log t + \log Z_t. \qquad (5)$$

The rate constant Z_t and the morphological exponent n'' can be obtained from the intercept and the slope of a plot of $\log[-\ln(1 - X(t))]$ versus logt. The final form of Z_t has to be corrected by considering the effect of the cooling rate:

$$\log Z_c = \log Z_t/\alpha \quad (6)$$

The results were reported in Table IV. Values of n'' ranged from 3.0 to 4.0. In the range of cooling rates, n'' does not change significantly with the cooling rate. The n'' of EP-*g*-GMA is higher than the n'' of pure EP. This is in accordance with the isothermal results. The rate constant Z_c reflects the crystallization kinetics and is equivalent to the Avrami rate constant in isothermal crystallization kinetics. Figure 7 shows that Z_c values of EP-*g*-GMA are higher than that of EP, and Z_c increases to a plateau of Z_c = 1.06–1.10 in the case of EP-*g*-GMA and Z_c = 0.90 in the case of EP.

CONCLUSION

Functionalization of EP led to an increase in crystallization temperatures of propylene sequences. It is attributed to the fact that the grafted GMA can act as a nucleating agent for crystallization of propylene sequences. The isothermal and nonisothermal crystallization kinetics showed that the Avrami exponent n and Ziabicki exponent n'' for EP-*g*-GMA were all higher than that for EP. The results of crystallization kinetics indicated that the grafting of GMA onto EP caused an increase in the crystallization rate of propylene sequences. This confirmed the previous conclusion.

We acknowledge the financial support of the Department of Material Sciences, National Natural Sciences Foundation of China, Project No. 59433010-01.

REFERENCES

1. I. Mondragon, M. Gaztelumendi, and J. Nazabal, *Polym. Eng. Sci.*, **26,** 1478 (1986).
2. I. Mongragon, M. Gazelumendi, and J. Nazabal, *Polym. Eng. Sci.*, **28,** 1126 (1988).
3. I. K. Mehta, S. Kumar, G. S. Chauhan, and B. N. Mishra, *J. Appl. Polym. Sci.*, **41,** 1171 (1990).
4. R. P. Scingh, *Prog. Polym. Sci.*, **17,** 251 (1992).
5. G. De Vito, G. Maglio, N. Lanzetta, M. Malinconico, P. Musto, and R. Palumbo, *J. Polym. Sci., Polym. Chem. Ed.*, **22,** 1334 (1984).
6. G. Ruggeri, A. Aglietto, A. Petragnani, and F. Ciardelli, *Eur. Polym. J.*, **19,** 863 (1983).
7. R. Greco, G. Maglio, E. Martuscelli, P. Musto, and R. Palumbo, *Polym. Proc. Eng.*, **2–4,** 273 (1986).
8. R. Greco, G. Maglio, and P. Musto, *J. Appl. Polym. Sci.*, **33,** 2531 (1987).
9. G. Bucci and T. Simonazzi, *Chim. Ind. (Milano)*, **44,** 262 (1962).
10. G. Maglio, F. Milani, P. Musto, and F. Riva, *Makromol. Chem. Rapid Comm.*, **8,** 589 (1987).
11. C. D. Han and H. K. Chuang, *J. Appl. Polym. Sci.*, **30,** 2431–2455 (1985).
12. C. C. Chen and J. L. White, *Polym. Eng. Sci.*, **33**(14), 923–930 (1993).
13. B. S. Chang, F. C. Chang, N. C. Chu, and C. S. Huang, *Proc. 15th R. O. C. Polym. Symp.*, Taiwan, 1992, p. 425.
14. C. T. Ma and F. C. Chang, *J. Appl. Polym. Sci.*, **49,** 913 (1993).
15. W. B. Liu and F. C. Chang, *Polym. Preprints*, **34**(2), 803 (1993).
16. F. C. Chang and Y. C. Hwu, *Polym. Eng. Sci.*, **31,** 1509 (1991).
17. X. M. Zhang, Z. H. Yin, J. H. Yin, *J. Appl. Polym. Sci.*, to appear.
18. N. Gaylord, M. Mehta, and R. Mehta, *J. Appl. Polym. Sci.*, **33,** 2549 (1987).
19. R. Greco, C. Mancarella, E. Martuscelli, G. Ragosta, and J. H. Yin, *Makromol. Chem.*, **188,** 2231 (1987).
20. M. Gordon and I. H. Hillier, *Phil. Mag.*, **11,** 31 (1965).
21. C. N. Velisaris and J. C. Seferis, *Polym. Eng. Sci.*, **26,** 1574 (1986).
22. T. Kowalewski and A. Galeski, *J. Appl. Polym. Sci.*, **32,** 2919 (1986).
23. L. Marker, P. M. Hay, G. P. Tilley, R. M. Early, and O. J. Sweeting, *J. Polym. Sci.*, **38,** 33 (1959).
24. J. H. Griffith and B. G. Ranby, *J. Polym. Sci.*, **38,** 107 (1959).
25. B. Wunderlich, in *Macromolecular Physics*, Vol. 2, Ch. 6, Academic Press, New York, 1976.
26. E. Martescelli, *Polym. Eng. Sci.*, **24,** 563 (1984).
27. M. L. Williams, R. F. Landel, and J. D. Feng, *J. Am. Chem. Soc.*, **77,** 3701 (1995).
28. J. I. Lauritzen and J. D. Hoffman, *J. Chem. Phys.*, **31,** 1680 (1959).
29. R. Greco, C. Mancarella, E. Martuscelli, G. Ragosta, and J. H. Yin, *Makromol. Chem.*, **188,** 2231 (1987).
30. H. N. Back and H. D. Ledbetter, *J. Appl. Polym. Sci.*, **9,** 2131 (1965).
31. J. D. Muzzy, D. G. Bright, and G. H. Hoyos, *Polym. Eng. Sci.*, **18,** 437 (1978).
32. A. Ziabicki, *Appl. Polym. Symp.*, **6,** 1 (1967).

Received December 12, 1995
Accepted June 21, 1996